other preface, just an insight

corrected
29/07/13

Chapter 1

Preface

The elementary modes of nuclear excitation are vibrations and rotations, single–particle (quasiparticle) motion, and pairing vibrations and rotations. The specific reactions probing these modes are inelastic ~~and Coulomb excitation~~, single– and two– particle transfer processes respectively.

Pairing vibrations and rotations, closely connected with nuclear superfluidity are, arguably, a paradigm of quantal nuclear phenomena. They thus play a central role within the field of nuclear structure. It is only natural that two–nucleon transfer plays a similar role concerning direct nuclear reactions. In fact, this is the central subject of the present monograph.

At the basis of pairing phenomena one finds Cooper pairs, weakly bound, extended, strongly overlapping bosonic entities, made out of pairs of nucleons dressed by collective vibrations and interacting through the exchange of these vibrations as well as through the bare NN–interaction. Cooper pairs not only change the statistics of the nuclear stuff around the Fermi surface and, condensing, the properties of nuclei close to their ground state. They also display a rather remarkable mechanism of tunnelling between target and projectile in direct two–nucleon transfer reaction. In fact, displaying correlations over distances (correlation length) much larger than nuclear dimensions, Cooper pairs are forced to be confined within such dimensions by the action of the average potential, which can be viewed as an external field as far as these pairs are concerned.

The correlation length paradigm comes into evidence, for example, when two nuclei are set into weak contact in a direct reaction. In this case, each of the partner nucleons has a finite probability to be confined within the mean field of each of the two nuclei. It is then natural that a Cooper pair can tunnel, equally well correlated, between target and projectile, through a simultaneous than through a successive transfer process. In particular, in this last case, making use of virtual states which, if forced to become real by intervening the reaction with an external mean field, will lead to single–nucleon transfer ~~processes~~. The above mentioned weak coupling Cooper pair tunnelling reminds the tunnelling mechanism of electronic Cooper pairs across a barrier (e.g. a dioxide layer) separating two superconductors, known as Josephson junction. The main difference is that, as a rule, in the nuclear time dependent junction provided by a direct two–nucleon transfer process, only one or even none of the two weakly interacting nuclei are superfluid (or superconducting). Now, in nuclei, paradigmatic example of fermionic finite many–body system, zero point fluctuation (ZPF) in general, and those associated with pair addition and pair substraction modes known as pairing

vibrations in particular, are much stronger than in condensed matter. Consequently, and in keeping with the fact that pairing vibrations are the nuclear embodiment of Cooper pairs in nuclei, pairing correlations based on even a single Cooper pair lead to clearly observable effects. In some cases, like for example in connection with the exotic nucleus ^{11}Li, to a tenuous halo extending much beyond standard nuclear dimensions.

Cooper pair tunnelling has played and is playing a central role in the probing of these subtle quantal phenomena, both in the case of exotic nuclei as well as of nuclei lying along the stability valley, and have been instrumental in shedding light on the subject of pairing in nuclei at large, and on nuclear superfluidity in particular. Consequently, the subject of two–nucleon transfer occupies a central place in the present monograph both concerning the conceptual and the computational aspects of the description of nuclear pairing, as well as regarding the quantitative confrontation of the results and predictions with the experimental findings.

Because the interweaving of the variety of elementary modes of nuclear excitation, the study of Cooper pair tunnelling in nuclei aside from requiring a consistent description of nuclear structure in terms of dressed quasiparticles and vibrations, resulting from both bare and induced interactions, involves also the description of one–nucleon transfer as well as knock out processes, let alone inelastic and Coulomb excitation processes. The corresponding softwares COOPER, ONE, KNOCK, INELASTIC and COULOMB are briefly presented, referring to the enclosed CD for the corresponding files and input–output examples.

Summing up, general physical arguments and technical computational details, as well as the software used in the description and calculation of the absolute two–nucleon transfer cross sections, making use of state of the art nuclear structure information, are provided. As a consequence, theoretical and experimental practitioners, as well as PhD students could use, at profit, the present monograph.

(a) Concerning the notation, we have divided each chapter into sections. Each subsection may in turn be broken down into subsection. Equations and Figures are identified by the number of the chapter and that of the section. Thus (6.1.33) labels the thitythird equation of Section 1 of Chapter 6. Similarly, Fig. 6.1.2 labels the second figure of Section 1 of chapter 6. Concerning the Appendices, they are labaled by the chapter number and by a Latin letter in alphabetic order, e.g. App. 6.A, App. 6.B, etc. Concerning equations and Figures, a sequential number is added. Thus (6.E.15) labels the fifteenth equation of appendix E of Chapter 6, while Fig 6.F.1 labels the first figure of appendix F of Chapter 6.

(a)

Gregory: no es posible hacer un formato con letras un poquito mas grande ??

ref.
Fig.
App.
Table

Chapter 6

One–particle transfer

(Chapters 7 and 8 (7: formalism two-nucleon transfer, 8: applications and examples))

and refs. therein

cf.

In what follows we present a derivation of the one–particle transfer differential cross section within the framework of the DWBA (Satchler, 1980; Broglia and Winther, 2004). The structure input for the calculations are mean field potentials and single–particle states dressed through the coupling with the variety of collective, (quasi) bosonic vibrations, leading to modified formfactors[1] resulting from the interweaving of these vibrations and a number of orbitals with the original, unperturbed single–particle state (Bohr and Mottelson, 1975; Bès and Broglia, 1977). With the help of these modified formfactors, and of optical potentials, one can calculate the absolute differential cross sections, quantities which can be directly compared with the experimental findings.

In this way one avoids to introduce, let alone use spectroscopic factors, quantities which are rather elusive to define. This is in keeping with the fact that as a nucleon moves through the nucleus it feels the presence of the other nucleons whose configurations change as time proceeds. It takes time for this information to be fed back on the nucleon. This renders the average potential nonlocal in time (cf. C. Mahaux et al. (1985) and references therein). A time–dependent operator can always be transformed into an energy dependent operator, implying an ω–dependence of the properties which are usually adscribed to particles like (effective) mass, charge, etc. Furthermore, due to the Pauli principle, the average potential is also non local in space (cf. App (??)). Consequently, one is forced to deal with nucleons which carry around a cloud of (quasi) bosons, aside from exchanging its position with that of the other nucleons. It is of notice that the above mentioned phenomena are not only found within the realm of nuclear physics, but are common within the framework of many–body systems as well as of field theories like quantum electrodynamic (QED). In fact, a basic result of such theories is that nothing is free (Feynman, 1975). A textbook example being provided by the Lamb shift, resulting from the dressing of the hydrogen atom electron, as a result of the exchange of this electron with those participating in the spontaneous, virtual excitation (zero point fluctuations (ZPF)) of the QED vacuum (cf. App (??)). Within this context see Sect. ??. (Examples and Applications) concerning the phenomenon of parity inversion in N=6 (closed shell) exotic halo nuclei.

(cf. Apps. A and B)

really

(cf. Apps. C and D)

6,2

the

of

transfer

renormalized

cf. e.g.

[1] It is of notice that single–particle modified formfactors have their counterpart in the transition densities (??) and in the modified two–nucleon formfactors (??) associated with inelastic and pair transfer (Broglia et al., 1973), respectively

with

reactions,

(Ch. 5 (inelastic scattering))

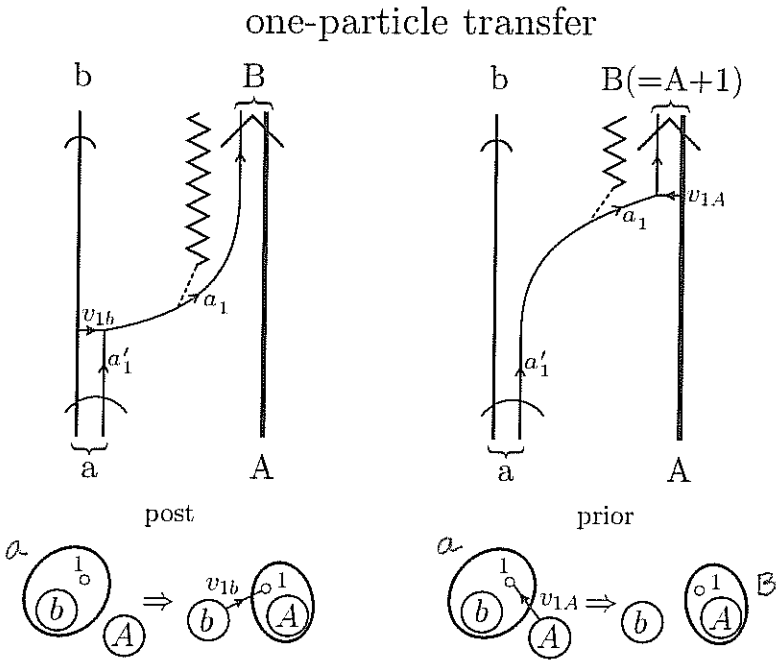

Figure 6.1.1: One–particle reaction $a(= b + 1) + A \rightarrow b + B(= A + 1)$. The time arrow is assumed to point upwards. The quantum numbers characterizing the states in which the transferred nucleon moves in projectile and target are denoted a'_1 and a_1 respectively. The interaction inducing the nucleon to be transferred can act either in the entrance channel ((a, A); v_{1A}, prior representation) or in the exit channel ((b, B); v_{1b}, post representation), in keeping with energy conservation. In the transfer process, the nucleon changes orbital at the same time that a change in the mass partition takes place. The corresponding relative motion mismatch is known as the recoil process, and is represented by a jagged line which provides information on the evolution of r_{1A} (r_{1b}). In other words on the coupling of reaction and transfer modes.

6.1 General derivation

6.1.1

We proceed now to derive the transition amplitude for the reaction (cf. Fig. 2)

$$A + a(= b + 1) \longrightarrow B(= A + 1) + b. \tag{6.1.1}$$

now

Let us assume that the nucleon bound initially to the core b is in a single–particle state with orbital and total angular momentum l_i and j_i respectively, and that the nucleon in the final state (bound to core A) is in the l_f, j_f state. The total spin and magnetic quantum numbers of nuclei A, a, B, b are $\{J_A, M_A\}, \{J_a, M_a\}, \{J_B, M_B\}, \{J_b, M_b\}$ respectively. Denoting ξ_A and ξ_b the intrinsic coordinates of the wavefunctions describing the structure of nuclei A and b ~~respectively~~, and $\mathbf{r}_{An}$ and $\mathbf{r}_{bn}$ the relative coordinates of the transferred nucleon with respect to the CM of nuclei A and b ~~respectively~~, one can

For a simplified version we refer to app. 6.E, while for an alternative derivation within the framework of knock-out reaction cf. App. 6.F.

write the "intrinsic" wavefunctions of the colliding nuclei A, a as

$$\begin{aligned}&\phi^{J_A}_{M_A}(\xi_A),\\ &\Psi(\xi_b, \mathbf{r}_{b1}) = \sum_{m_i}\langle J_b\ j_i\ M_b\ m_i|J_a\ M_a\rangle\phi^{J_b}_{M_b}(\xi_b)\psi^{j_i}_{m_i}(\mathbf{r}_{bn}, \sigma),\end{aligned} \tag{6.1.2}$$

while the "intrinsic" wavefunctions describing the structure of nuclei B and b are

$$\begin{aligned}&\phi^{J_b}_{M_b}(\xi_b),\\ &\Psi(\xi_A, \mathbf{r}_{A1}) = \sum_{m_f}\langle J_A\ j_f\ M_A\ m_f|J_B\ M_B\rangle\phi^{J_A}_{M_A}(\xi_A)\psi^{j_f}_{m_f}(\mathbf{r}_{An}, \sigma).\end{aligned} \tag{6.1.3}$$

For an unpolarized incident beam (sum over M_A, M_a and divide by $(2J_A+1), (2J_a+1)$) and assuming that one does not detect the final polarization (sum over M_B, M_b), the differential cross section in the DWBA can be written as

$$\begin{aligned}\frac{d\sigma}{d\Omega} = &\frac{k_f}{k_i}\frac{\mu_i\mu_f}{4\pi^2\hbar^4}\frac{1}{(2J_A+1)(2J_a+1)}\\ &\times\sum_{\substack{M_A,M_a\\M_B,M_b}}\left|\sum_{m_i,m_f}\langle J_b\ j_i\ M_b\ m_i|J_a\ M_a\rangle\langle J_A\ j_f\ M_A\ m_f|J_B\ M_B\rangle T_{m_i,m_f}\right|^2.\end{aligned} \tag{6.1.4}$$

The transition amplitude T_{m_i,m_f} is

$$T_{m_i,m_f} = \sum_\sigma\int d\mathbf{r}_f d\mathbf{r}_{bn}\chi^{(-)*}(\mathbf{r}_f)\psi^{j_f*}_{m_f}(\mathbf{r}_{An}, \sigma)V(r_{bn})\psi^{j_i}_{m_i}(\mathbf{r}_{bn}, \sigma)\chi^{(+)}(\mathbf{r}_i), \tag{6.1.5}$$

where

$$\psi^{j_i}_{m_i}(\mathbf{r}_{An}, \sigma) = u_{j_i}(r_{bn})\left|Y^{l_i}(\hat{r}_i)\chi(\sigma)\right|_{j_i m_i} \tag{6.1.6}$$

is the single–particle wavefunction describing the motion of the nucleon to be transferred, in the initial state. Similarly for $\psi^{j_f}_{m_f}$. The incoming and outgoing distorted waves are

$$\chi^{(+)}(\mathbf{k}_i, \mathbf{r}_i) = \frac{4\pi}{k_i r_i}\sum_{l'} i^{l'}e^{i\sigma^{l'}_i}g_{l'}(\hat{r}_i)\left[Y^{l'}(\hat{r}_i)Y^{l'}(\hat{k}_i)\right]^0_0, \tag{6.1.7}$$

and

$$\chi^{(-)*}(\mathbf{k}_f, \mathbf{r}_f) = \frac{4\pi}{k_f r_f}\sum_l i^{-l}e^{i\sigma^l_f}f_l(\hat{r}_f)\left[Y^l(\hat{r}_f)Y^l(\hat{k}_f)\right]^0_0, \tag{6.1.8}$$

respectively. Now,

$$\begin{aligned}\left[Y^l(\hat{r}_f)Y^l(\hat{k}_f)\right]^0_0\left[Y^{l'}(\hat{r}_i)Y^{l'}(\hat{k}_i)\right]^0_0 = &\sum_K((ll)_0(l'l')_0|(ll')_K(ll')_K)_0\\ &\times\left\{\left[Y^l(\hat{r}_f)Y^{l'}(\hat{r}_i)\right]^K\left[Y^l(\hat{k}_f)Y^{l'}(\hat{k}_i)\right]^K\right\}^0_0.\end{aligned} \tag{6.1.9}$$

The $9j$–symbol can be explicitly evaluated to give,

$$((ll)_0(l'l')_0|(ll')_K(ll')_K)_0 = \sqrt{\frac{2K+1}{(2l+1)(2l'+1)}}, \tag{6.1.10}$$

while the coupled expression can be written as

and the angular momenta coupling is

$$\left\{ \left[Y^l(\hat{r}_f)Y^{l'}(\hat{r}_i)\right]^K \left[Y^l(\hat{k}_f)Y^{l''}(\hat{k}_i)\right]^K \right\}_0^0 = \sum_M \langle K\ K\ M\ -M|0\ 0\rangle \left[Y^l(\hat{r}_f)Y^{l''}(\hat{r}_i)\right]_M^K$$
$$\times \left[Y^l(\hat{k}_f)Y^{l''}(\hat{k}_i)\right]_{-M}^K = \sum_M \frac{(-1)^{K+M}}{\sqrt{2K+1}} \left[Y^l(\hat{r}_f)Y^{l'}(\hat{r}_i)\right]_M^K \left[Y^l(\hat{k}_f)Y^{l''}(\hat{k}_i)\right]_{-M}^K . \tag{6.1.11}$$

Thus,

$$\left[Y^l(\hat{r}_f)Y^l(\hat{k}_f)\right]_0^0 \left[Y^{l'}(\hat{r}_i)Y^{l'}(\hat{k}_i)\right]_0^0 =$$
$$\sum_{K,M} \frac{(-1)^{K+M}}{\sqrt{(2l+1)(2l'+1)}} \left[Y^l(\hat{r}_f)Y^{l'}(\hat{r}_i)\right]_M^K \left[Y^l(\hat{k}_f)Y^{l'}(\hat{k}_i)\right]_{-M}^K . \tag{6.1.12}$$

For the angular integral to be different from zero, the integrand must be coupled to zero angular momentum (scalar). Noting that the only variables over which one integrates in the above expression are $\hat{r}_i, \hat{r}_f$, we have to couple the remaining functions of the angular variables, namely the wavefunctions $\psi^{j_f *}_{m_f}(\mathbf{r}_{An}, \sigma) = (-1)^{j_f - m_f}\psi^{j_f}_{-m_f}(\mathbf{r}_{An}, -\sigma)$ and $\psi^{j_i}_{m_i}(\mathbf{r}_{bn}, \sigma)$ to angular momentum K, as well as to fulfill $M = m_f - m_i$. Let us then consider

? ? Gregory

$\sigma = m_s = \pm 1/2$

$\chi^{1/2}(-\sigma)$

$$(-1)^{j_f - m_f}\psi^{j_f}_{-m_f}(\mathbf{r}_{An}, -\sigma)\psi^{j_i}_{m_i}(\mathbf{r}_{bn}, \sigma) = (-1)^{j_f - m_f} u_{j_f}(r_{An})u_{j_i}(r_{bn})$$
$$\times \sum_P \langle j_f\ j_i\ -m_f\ m_i|P\ m_i - m_f\rangle \left\{ \left[Y^{l_f}(\hat{r}_{An})\chi^{1/2}(-\sigma)\right]^{j_f} \left[Y^{l_i}(\hat{r}_{bn})\chi^{1/2}(\sigma)\right]^{j_i} \right\}_{m_i - m_f}^P . \tag{6.1.13}$$

Recoupling the spherical harmonics to angular momentum K and the spinors to $S = 0$, only one term survives the angular integral in (6.1.5), namely

$$(-1)^{j_f - m_f} u_{j_f}(r_{An})u_{j_i}(r_{bn})((l_f \tfrac{1}{2})_{j_f}(l_i \tfrac{1}{2})_{j_i}|(l_f l_i)_K(\tfrac{1}{2}\tfrac{1}{2})_0)_K$$
$$\times \langle j_f\ j_i\ -m_f\ m_i|K\ m_i - m_f\rangle \left[Y^{l_f}(\hat{r}_{An})Y^{l_i}(\hat{r}_{bn})\right]_{m_i - m_f}^K \left[\chi(-\sigma)\chi(\sigma)\right]_0^0 . \tag{6.1.14}$$

Making use of the fact that the sum over spins yields a factor $-\sqrt{2}$, and in keeping with the fact that $M = m_f - m_i$, one obtains,

$$T_{m_i, m_f} = (-1)^{j_f - m_f} \frac{-16\sqrt{2}\pi^2}{k_f k_i} \sum_{ll'} i^{l'-l} e^{\sigma^l_f + \sigma^{l'}_i} \sum_K ((l_f \tfrac{1}{2})_{j_f}(l_i \tfrac{1}{2})_{j_i}|(l_f l_i)_K(\tfrac{1}{2}\tfrac{1}{2})_0)_K$$
$$\times \langle j_f\ j_i\ -m_f\ m_i|K\ m_i - m_f\rangle \left[Y^l(\hat{k}_f)Y^{l'}(\hat{k}_i)\right]_{m_i - m_f}^K \int d\mathbf{r}_f d\mathbf{r}_{bn} \frac{f_l(r_f)g_{l'}(r_i)}{r_f r_i}$$
$$\times u_{j_f}(r_{An})u_{j_i}(r_{bn})V(r_{bn})(-1)^{K+m_f-m_i} \left[Y^l(\hat{r}_f)Y^{l'}(\hat{r}_i)\right]_{m_f - m_i}^K \left[Y^{l_f}(\hat{r}_{An})Y^{l_i}(\hat{r}_{bn})\right]_{m_i - m_f}^K . \tag{6.1.15}$$

Again, the only term of the expression

$$(-1)^{K+m_f-m_i} \left[Y^l(\hat{r}_f)Y^{l'}(\hat{r}_i)\right]_{m_f - m_i}^K \left[Y^{l_f}(\hat{r}_{An})Y^{l_i}(\hat{r}_{bn})\right]_{m_i - m_f}^K =$$
$$(-1)^{K+m_f-m_i} \sum_P \langle K\ K\ m_f - m_i\ m_i - m_f|P\ 0\rangle \left\{ \left[Y^l(\hat{r}_f)Y^{l'}(\hat{r}_i)\right]^K \left[Y^{l_f}(\hat{r}_{An})Y^{l_i}(\hat{r}_{bn})\right]^K \right\}_0^P$$

which survives after angular integration is the one with $P = 0$, that is,

$$\frac{1}{\sqrt{(2K+1)}}\left\{\left[Y^{l}(\hat{r}_f)Y^{l'}(\hat{r}_i)\right]^{K}\left[Y^{l_f}(\hat{r}_{An})Y^{l_i}(\hat{r}_{bn})\right]^{K}\right\}_{0}^{0} =$$

$$\frac{1}{\sqrt{(2K+1)}}\sum_{M_K}\langle K\ K\ M_K\ -M_K|0\ 0\rangle\left[Y^{l}(\hat{r}_f)Y^{l'}(\hat{r}_i)\right]_{M_K}^{K}$$

$$\times\left[Y^{l_f}(\hat{r}_{An})Y^{l_i}(\hat{r}_{bn})\right]_{-M_K}^{K} = \frac{1}{\sqrt{(2K+1)}}\sum_{M_K}\frac{(-1)^{K+M_K}}{\sqrt{(2K+1)}}\left[Y^{l}(\hat{r}_f)Y^{l'}(\hat{r}_i)\right]_{M_K}^{K}$$

$$\times\left[Y^{l_f}(\hat{r}_{An})Y^{l_i}(\hat{r}_{bn})\right]_{-M_K}^{K} =$$

$$\frac{1}{2K+1}\sum_{M_K}(-1)^{K+M_K}\left[Y^{l}(\hat{r}_f)Y^{l'}(\hat{r}_i)\right]_{M_K}^{K}\left[Y^{l_f}(\hat{r}_{An})Y^{l_i}(\hat{r}_{bn})\right]_{-M_K}^{K},$$

an expression which is spherically symmetric. One can evaluate it for a particular configuration, in particular setting $\hat{r}_f = \hat{z}$ and the center of mass A, b, n in the $x - z$ plane (see Fig. 6.E.1). Once the orientation in space of this "standard" configuration is specified (with, for example, a rotation $0 \le \alpha \le 2\pi$ around $\hat{z}$, a rotation $0 \le \beta \le \pi$ around the new x axis and a rotation $0 \le \gamma \le 2\pi$ around $\hat{r}_{bB}$), the only remaining angular coordinate is θ, while the integral over the other three angles yields a $8\pi^2$. Setting $\hat{r}_f = \hat{z}$ one obtains

$$\left[Y^{l}(\hat{r}_f)Y^{l'}(\hat{r}_i)\right]_{M_K}^{K} = \langle l\ l'\ 0\ M_K|K\ M_K\rangle\sqrt{\frac{2l+1}{4\pi}}Y_{M_K}^{l'}(\hat{r}_i). \tag{6.1.16}$$

Because of $M = m_i - m_f$ and $m = m_f$, $T_{m_i,m_f} \equiv T_{m,M}$ where

$$T_{m,M} = (-1)^{j_f-m}\frac{-64\sqrt{2}\pi^{7/2}}{k_f k_i}\sum_{ll'}i^{l'-l}e^{\sigma_f^{l}+\sigma_i^{l'}}\sqrt{2l+1}\sum_{K}\frac{(-1)^{K}}{2K+1}((l_f\tfrac{1}{2})_{j_f}(l_i\tfrac{1}{2})_{j_i}|(l_f l_i)_K(\tfrac{1}{2}\tfrac{1}{2})_0)_K$$

$$\times\langle j_f\ j_i\ -m\ M+m|K\ M\rangle\left[Y^{l}(\hat{k}_f)Y^{l'}(\hat{k}_i)\right]_{M}^{K}\int d\mathbf{r}_f d\mathbf{r}_{bn}\frac{f_l(r_f)g_{l'}(r_i)}{r_f r_i}$$

$$\times u_{j_f}(r_{An})u_{j_i}(r_{bn})V(r_{bn})\sum_{M_K}(-1)^{M_K}\langle l\ l'\ 0\ M_K|K\ M_K\rangle\left[Y^{l_f}(\hat{r}_{An})Y^{l_i}(\hat{r}_{bn})\right]_{-M_K}^{K}Y_{M_K}^{l'}(\hat{r}_i). \tag{6.1.17}$$

We now turn our attention to the sum

$$\sum_{\substack{M_A,M_a\\M_B,M_b}}\left|\sum_{m,M}\langle J_b\ j_i\ M_b\ m_i|J_a\ M_a\rangle\langle J_A\ j_f\ M_A\ m_f|J_B\ M_B\rangle T_{m,M}\right|^2, \tag{6.1.18}$$

found in the expression for the differential cross section (6.1.4). For any given value m', M' of m, M, the sum will be

$$\sum_{M_a,M_b}|\langle J_b\ j_i\ M_b\ m_i|J_a\ M_a\rangle|^2\sum_{M_A,M_B}\left|\langle J_A\ j_f\ M_A\ m_f|J_B\ M_B\rangle\right|^2\left|T_{m',M'}\right|^2 =$$

$$\frac{(2J_a+1)(2J_B+1)}{(2j_i+1)(2j_f+1)}\sum_{M_a,M_b}|\langle J_b\ J_a\ M_b\ -M_a|j_i\ m_i\rangle|^2$$

$$\times\sum_{M_A,M_B}\left|\langle J_A\ J_B\ M_A\ -M_B|j_f\ m_f\rangle\right|^2\left|T_{m',M'}\right|^2, \tag{6.1.19}$$

by virtue of the symmetry property of Clebsch–Gordan coefficients

$$\langle J_b\ j_i\ M_b\ m_i|J_a\ M_a\rangle = (-1)^{J_b-M_b}\sqrt{\frac{(2J_a+1)}{(2j_i+1)}}\langle J_b\ J_a\ M_b\ -M_a|j_i\ m_i\rangle. \tag{6.1.20}$$

The sum over the Clebsch–Gordan coefficients in (6.1.19)is one, so (6.1.18) is just

$$\frac{(2J_a+1)(2J_B+1)}{(2j_i+1)(2j_f+1)}\sum_{m,M}\left|T_{m,M}\right|^2, \tag{6.1.21}$$

and the differential cross section turns out to be

$$\frac{d\sigma}{d\Omega} = \frac{k_f}{k_i}\frac{\mu_i\mu_f}{4\pi^2\hbar^4}\frac{(2J_B+1)}{(2j_i+1)(2j_f+1)(2J_A+1)}\sum_{m,M}\left|T_{m,M}\right|^2. \tag{6.1.22}$$

where

$$T_{m,M} = \sum_{Kll'}(-1)^{-m}\langle j_f\ j_i\ -m\ M+m|K\ M\rangle\left[Y^l(\hat{k}_f)Y^{l'}(\hat{k}_i)\right]^K_M t^K_{ll'}. \tag{6.1.23}$$

Orienting $\hat{k}_i$ along the incident z direction leads to,

$$\left[Y^l(\hat{k}_f)Y^{l'}(\hat{k}_i)\right]^K_M = \langle l\ l'\ M\ 0|K\ M\rangle\sqrt{\frac{2l'+1}{4\pi}}Y^l_M(\hat{k}_f), \tag{6.1.24}$$

and

$$T_{m,M} = \sum_{Kll'}(-1)^{-m}\langle l\ l'\ M\ 0|K\ M\rangle\langle j_f\ j_i\ -m\ M+m|K\ M\rangle Y^l_M(\hat{k}_f)\,t^K_{ll'}, \tag{6.1.25}$$

with

$$\begin{aligned} t^K_{ll'} = (-1)^{K+j_f}\frac{-32\sqrt{2}\pi^3}{k_fk_i}i^{l'-l}e^{\sigma^l_f+\sigma^{l'}_i}\frac{\sqrt{(2l+1)(2l'+1)}}{2K+1}((l_f\tfrac{1}{2})_{j_f}(l_i\tfrac{1}{2})_{j_i}|(l_fl_i)_K(\tfrac{1}{2}\tfrac{1}{2})_0)_K \\ \times\int dr_f\,dr_{bn}d\theta r^2_{bn}\sin\theta\, r_f\frac{f_i(r_f)g_{l'}(r_i)}{r_i}u_{j_f}(r_{An})u_{j_i}(r_{bn})V(r_{bn}) \\ \times\sum_{M_K}(-1)^{M_K}\langle l\ l'\ 0\ M_K|K\ M_K\rangle\left[Y^{l_f}(\hat{r}_{An})Y^{l_i}(\hat{r}_{bn})\right]^K_{-M_K}Y^{l'}_{M_K}(\hat{r}_i). \end{aligned} \tag{6.1.26}$$

6.1.1 Coordinates

6.1.2

To perform the integral in (6.1.26), one needs the expression of $r_i, r_{An}, \hat{r}_{An}, \hat{r}_{bn}, \hat{r}_i$ in term of the integration variables r_f, r_{bn}, θ.Because one is interested in evaluating these quantities in the particular configuration depicted in Fig. 6.1.1, one has

$$\mathbf{r}_f = r_f\,\hat{z}, \tag{6.1.27}$$

$$\mathbf{r}_{bn} = -r_{bn}(\sin\theta\,\hat{x}+\cos\theta\,\hat{z}), \tag{6.1.28}$$

$$\mathbf{r}_{Bn} = \mathbf{r}_f+\mathbf{r}_{bn} = -r_{bn}\sin\theta\,\hat{x}+(r_f-r_{bn}\cos\theta)\,\hat{z}. \tag{6.1.29}$$

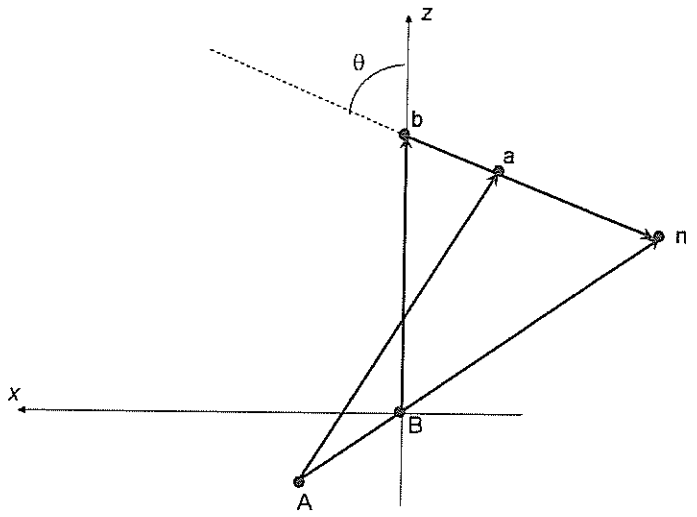

Figure 6.1.2: Coordinate system in the "standard" configuration. Note that $\mathbf{r}_f \equiv \mathbf{r}_{Bb}$, and $\mathbf{r}_i \equiv \mathbf{r}_{Aa}$.

One can then write

$$\mathbf{r}_{An} = \frac{A+1}{A}\mathbf{r}_{Bn} = -\frac{A+1}{A} r_{bn} \sin\theta\,\hat{x} + \frac{A+1}{A}(r_f - r_{bn}\cos\theta)\,\hat{z}, \tag{6.1.30}$$

$$\mathbf{r}_{an} = \frac{b}{b+1}\mathbf{r}_{bn} = -\frac{b}{b+1} r_{bn}(\sin\theta\,\hat{x} + \cos\theta\,\hat{z}), \tag{6.1.31}$$

and

$$\mathbf{r}_i = \mathbf{r}_{An} - \mathbf{r}_{an} = -\frac{2A+1}{(A+1)A} r_{bn}\sin\theta\,\hat{x} + \left(\frac{A+1}{A} r_f - \frac{2A+1}{(A+1)A} r_{bn}\cos\theta\right)\hat{z}, \tag{6.1.32}$$

where A, b are the number of nucleons of nuclei A and b respectively.

6.1.2 Zero range approximation

In the zero range approximation,

$$\int dr_{bn} r_{bn}^2 u_{j_i}(r_{bn}) V(r_{bn}) = D_0; \quad u_{j_i}(r_{bn}) V(r_{bn}) = \delta(r_{bn})/r_{bn}^2. \tag{6.1.33}$$

It can be shown (see Fig. 6.1.1) that for $r_{bn} = 0$

$$\mathbf{r}_{An} = \frac{m_A + 1}{m_A}\mathbf{r}_f, \qquad \mathbf{r}_i = \frac{m_A + 1}{m_A}\mathbf{r}_f. \tag{6.1.34}$$

One then obtains

$$t_{ll'}^{K} = \frac{-16\sqrt{2}\pi^2}{k_f k_i}(-1)^K \frac{D_0}{\alpha} i^{l'-l} e^{\sigma_f^{l'}+\sigma_i^{l}} \frac{\sqrt{(2l+1)(2l'+1)(2l_i+1)(2l_f+1)}}{2K+1} ((l_f\tfrac{1}{2})_{j_f}(l_i\tfrac{1}{2})_{j_i}|(l_f l_i)_K(\tfrac{1}{2}\tfrac{1}{2})_0)_K$$
$$\times \langle l\, l'\, 0\, 0|K\, 0\rangle\langle l_f\, l_i\, 0\, 0|K\, 0\rangle \int dr_f\, f_i(r_f) g_{l'}(\alpha r_f) u_{j_f}(\alpha r_f), \tag{6.1.35}$$

with

$$\alpha = \frac{A+1}{A}. \tag{6.1.36}$$

6.2 Examples and Applications

In this section we discuss some examples which illustrate the workings of single–particle transfer processes at large, and in particular the flavour of the limitations by which nuclear structure studies suffer, when this specific probe to study quasiparticle properties is not operative. Let us in fact start with such an example.

6.2.1 Dressing of single–particle states: parity inversion in ^{11}Li

The $N = 6$ isotope of $^{9}_{3}$Li displays quite ordinary structural properties and can, at first glance, be thought of a twoneutron hole system in the $N = 8$ closed shell. That this is not the case emerges clearly from the fact that ^{10}Li is not bound, the lowest virtual $(1/2^+)$ and resonant $(1/2^-)$ states testify to the fact that, in the present case, the $N = 6$ is a far better magic neutron number than $N = 8$. Furthermore, that the unbound $s_{1/2}$ state lies lower than the unbound $p_{1/2}$ state, in plain contradiction with static mean field theory. Dressing the (standard) mean field single–particle states with vibrations , mostly with the core quadrupole vibration, through polarization (effective masslike) and correlation diagrams (vacuum zero point fluctuations (ZPF)) diagrams, similar to those associated with the (lowest order) Lamb shift Feynman diagrams), move the $s_{1/2}$ and $p_{1/2}$ mean field levels around. In particular the $p_{1/2}$ from a bound state (≈ -1.2MeV) to a resonant state lying at ≈ 0.5 MeV (Pauli principle, vacuum ZPF process)

How can one check that CO and PO like processes as the ones shown in Fig. 22 (cf. also Fig. 22) are the basic processes dressing the odd neutron of ^{10}Li, and thus the mechanism at the basis of parity inversion? The answer is, forcing these virtual processes to become real. While this is not easy to accomplish in one–particle transfer processes involving the unbound $s_{1/2}$ and $p_{1/2}$, ^{10}Li virtual and resonant states, it can done with the help of two–particle transfer processes, namely that associated with inverse kinematics (p, t) reaction ^{1}H(^{11}Li,^{9}Li(2.69MeV; $1/2^-$))^{3}H (cf. Fig. 22 and Chs. 22). Such a reaction is feasible, in keeping with the fact that, adding a neutron to ^{10}Li leads to a bound state (see Fig. 22). In fact, $^{11}_{3}$Li$_8$ displays a two–neutron separation energy $S_{2n} \approx 400$ keV (for further details we refer to Ch. 22, Sect. 22). The price to pay for not being able to use the specific probe for single–particle modes (one–particle transfer), is that of adding to the self–energy contributions in question those corresponding to vertex corrections (cf. Fig. 22; for details cf. Sect. 22 (application $2n$–transfer)). Within the present context, it is difficult if not impossible to talk about single–particle motion without also referring to collective vibrational states

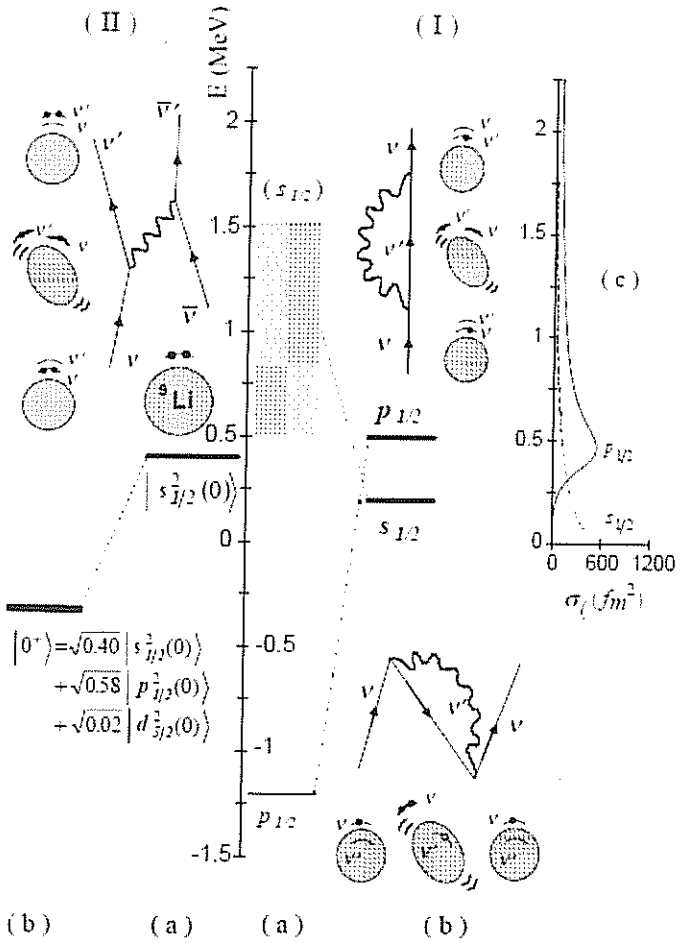

Figure 6.1.3: (I) Single-particle neutron resonances in ^{10}Li. In (a) the position of the levels $s_{1/2}$ and $p_{1/2}$ calculated making use of mean-field theory is shown (hatched area and thin horizontal line, respectively). The coupling of a single-neutron (upward pointing arrowed line) to a vibration (wavy line) calculated making use of the Feynman diagrams displayed in (b) (schematically depicted also in terms of either solid dots (neutron) or open circles (neutron hole) moving in a single-particle level around or in the ^{9}Li core (hatched area)), leads to conspicuous shifts in the energy centroid of the $s_{1/2}$ and $p_{1/2}$ resonances (shown by thick horizontal lines) and eventually to an inversion in their sequence. In (c) we show the calculated partial cross-section l for neutron elastic scattering off ^{9}Li. (II) The two-neutron system ^{11}Li. We show in (a) the meanfield picture of ^{11}Li, where two neutrons (solid dots) move in time-reversal states around the core ^{9}Li (hatched area) in the $s_{1/2}$ resonance leading to an unbound $s^2_{1/2}(0)$ state where the two neutrons are coupled to zero angular momentum. The exchange of vibrations between the two neutrons shown in the upper part of the figure leads to a density-dependent interaction which, added to the nucleon-nucleon interaction, correlates the two-neutron system leading to a bound state $|0^+\rangle$, where the two neutrons move with probability 0.40, 0.58 and 0.02 in the two-particle configurations $s^2_{1/2}(0)$, $p^2_{1/2}(0)$ and $d^2_{5/2}(0)$, respectively.

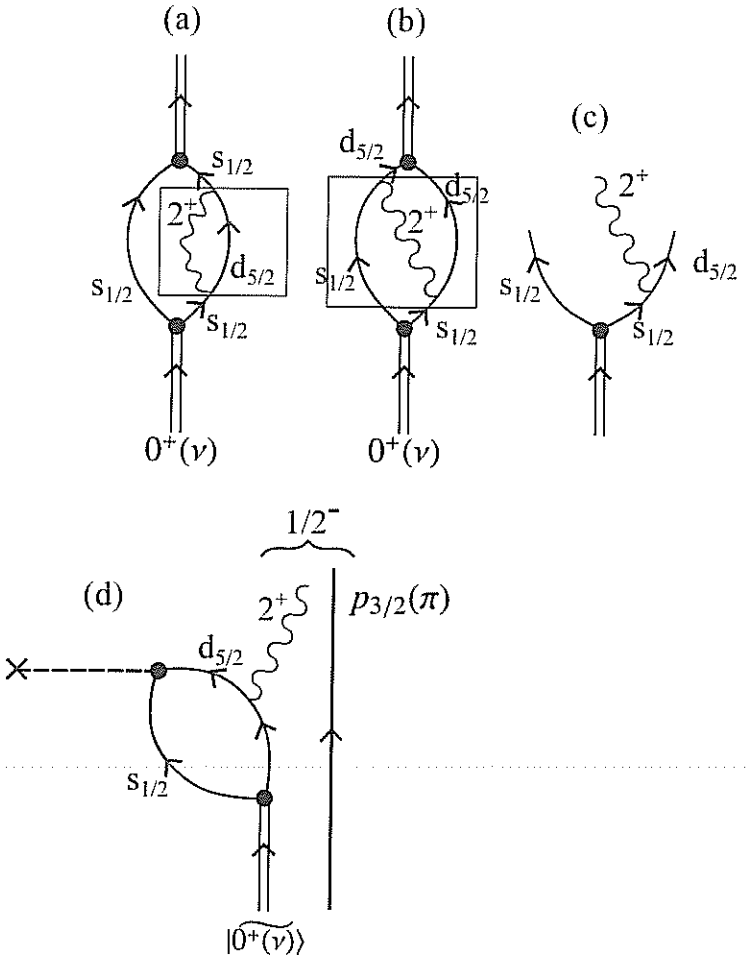

Figure 6.1.4: (a)Self–energy (see boxed process) and (b) vertex (pairing induced interaction boxed process) renormalization process, both associate with (c) a (two–particle)–(quadrupole vibration) intermediate (virtual state) which can be forced to became real in a (p,t) reaction ^{1}H(^{11}Li,^{9}Li)^{3}H exciting the first excited state $|2.69\text{MeV};1/2^-\rangle$ of ^{9}Li (see Ch.??.)

8 (examples and applications two-nucleon transfer)

6.2.2 $^{132}Sn(d,p)^{133}Sn$ and $^{132}Sn(p,d)^{131}Sn$ reactions

6.2.3 $^{120}Sn(d,p)^{121}Sn$ and $^{120}Sn(p,d)^{119}Sn$ reactions

6.1.3(II)

(in connection of both structure and reaction processes. Similarly, 6.1.4(a) and (b))

(cf. e.g. Fig. 6) ~~both in structure and reactions as well as~~ to talk about pair addition and pair substraction correlations, without at the same time talking about vibrations and dressed quasiparticle motion (see e.g. Fig. 5), ~~And this~~ again in structure and reactions. Within the framework of the present monograph, the above facts imply that Chapters 7 (inelastic), 8 (one–particle transfer) and 9 and 10 (two–particle transfer and applications) form a higher unity. ~~The unity extending~~ also to ~~Ch.~~ 11 (knock–out reactions), if one also considers the question of final state interactions, and thus of the possibility that the population of the state $1/2^-$ depicted in Fig. 5 receives contributions other, and more involved, than those associated with the direct two–nucleon pick–up depicted (for details cf. Ch. 8; cf. also Potel et al (2010)).

(concerning both; the content of App. F; 6.1.4(d); this unity extends; excited)

Appendix 6.A Minimal requirements for a consistent mean field theory

In what follows th question of why, rigorously speaking, one cannot talk about single–particle motion, let alone spectroscopic factor, not even within the framework of Hartree–Fock theory, is briefly touched upon. (6.A.1)

As can be seen from Fig. 1 the minimum requirements of selfconsistency to be imposed upon single particle motion requires both non–locality in space (HF) and in time (TDHF)

$$i\hbar\frac{\partial\rho_\nu}{\partial t} = -\frac{\hbar^2}{2m}\nabla^2\varphi_\nu(x,t) + \int dx'dt'\,U(x-x',t-t')\varphi_\nu(x',t'), \qquad (6.A.1)$$

and consequently also of collective vibrations and, consequently, from their interweaving to dressed single–particles (quasiparticles), let alone renormalized collective modes. Assuming for simplicity infinite nuclear matter (confined by a constant potential of depth V_0), and thus plane wave solutions, the above time–dependent Schrödinger equation leads to the quasiparticle dispersion relation (cf. e.g. 22)

(Brink and Broglia, 2005)

$$\hbar\omega = \frac{\hbar^2k^2}{2m^*} + \frac{m}{m^*}V_0, \qquad (6.A.2)$$

where the effective mass

$$m^* = \frac{m_k m_\omega}{m}, \qquad (6.A.3)$$

in the product of the k–mass

$$m_k = m\left(1 + \frac{m}{\hbar^2 k}\frac{\partial U}{\partial k}\right)^{-1} \qquad (6.A.4)$$

closely connected with the Pauli principle $\left(\frac{\partial U}{\partial k} \approx \frac{\partial U_+}{\partial k}\right)$, while the ω–mass

$$m_\omega = m\left(1 - \frac{\partial U}{\partial\hbar\omega}\right) \qquad (6.A.5)$$

(6.A.2)

results from the dressing of the nucleon through the coupling with the (quasi) bosons. Because typically $m_k \approx 0.7m$ and $m_\omega \approx 1.4m$ $m^* \approx m$, one could be tempted to conclude that the results embodied in the dispersion relation 22 reflects that the distribution of levels around the Fermi energy can be described in terms of the solutions of

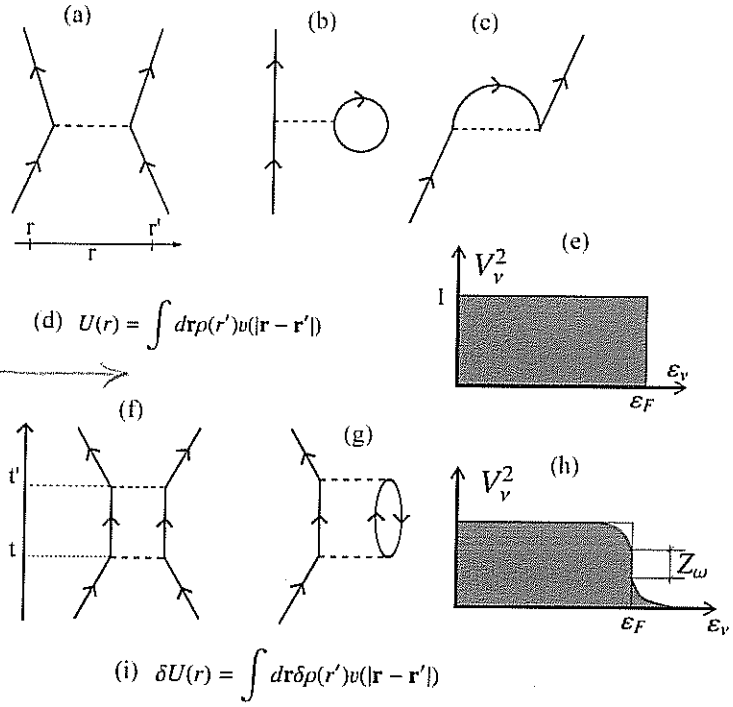

Figure 6.A.1: (a)Scattering of two nucleons through the bare *NN* interaction $v|\mathbf{r}-\mathbf{r}'|$, (b) contribution to the direct (U_v,Hartree) and (c) to the exchange (U_x, Fock) potential, resulting in (d) the (static) self consistent relation between potential and density, which (e) uncouples occupied ($\varepsilon_\nu \leq \varepsilon_F$) from empty states ($\varepsilon_\nu > \varepsilon_F$), (f) multiple scattering of two nucleons lead, through processes like the one depicted in (g), eventually propagated to all orders, to: (h) softening of the discontinuity of the occupancy of levels at ε_F, as well as to: (i) generalization of the static selfconsistency into a dynamic relation encompassing also collective vibrations (Time–dependent HF solutions of the nuclear Hamiltonian, conserving energy weighted sum rules).

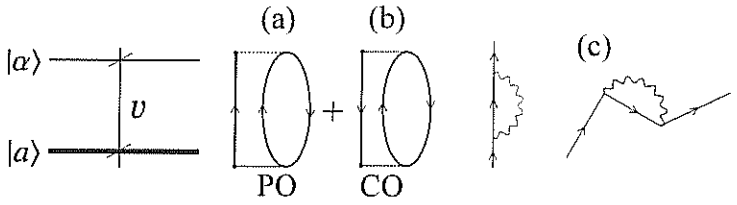

Figure 6.B.1: Two state schematic model describing the breaking of the strength of the pure single–particle state $|a\rangle$, through the coupling to collective vibrations (wavy line) associated with polarization (PO) and correlation (CO) processes.

a Schrödinger equation in which nucleons of mass equal to the bare nucleon mass m move in a Saxon–Woods potential of depth V_0.

Now, it can be shown that the occupancy of levels around ε_F is given by Z_ω (cf. Fig. 22) a quantity which is equal to $m/m_\omega \approx 0.7$. This, in keeping with the fact that the time the nucleon is coupled to the vibrations it cannot behave as a single–particle and can thus not contribute to e.g. the single–particle pickup cross section.

It is of notice that the selfconsistence requirements for the iterative solution of the Kohn–Sham equations

$$H^{KS}\varphi_\gamma(\mathbf{r}) = \lambda_\gamma\varphi_\gamma(\mathbf{r}), \tag{6.A.6}$$

where

$$H^{KS} = -\frac{\hbar^2}{2m_e}\nabla^2 + U_H(\mathbf{r}) + V_{ext}(\mathbf{r}) + U_{xc}(\mathbf{r}), \tag{6.A.7}$$

H^{KS} being known as the Kohn–Sham Hamiltonian, $V_{ext}(\mathbf{r})$ being the field created by the ions and acting on the electrons. Both the Hartree and the exchange–correlation potentials $U_H(\mathbf{r})$ and $U_{xc}(\mathbf{r})$ depend on the (local) density, hence on the whole set of wavefunctions $\varphi_\gamma(\mathbf{r})$. Thus, the set of KS–equations must be solve selfconsistently (cf. e.g. Broglia et al (2004) and refs. therein)

Appendix 6.B Model for single–particle strength function: Dyson equation

In the previous section we introduced the argument of the impossibility of defining a "bona fide" single–particle spectroscopic factor. It was done with the help of Feynman (NFT) diagrams. In what follows we essentially repeat the arguments, but this time in terms of Dyson's (Schwinger) language. For simplicity, we consider a two–level model where the pure single–particle state $|a\rangle$ couples to a more complicated state $|\alpha\rangle$, made out of a fermion (particle or hole), couple to a particle–hole excitation which, if iterated to all orders can give rise to a collective state (cf. Fig. 22). The Hamiltonian describing the system is

$$H = H_0 + U \tag{6.B.1}$$

where

$$H_0|a\rangle = E_a|a\rangle, \tag{6.B.2}$$

and

$$H_0|\alpha\rangle = E_\alpha|\alpha\rangle. \tag{6.B.3}$$

Let us call $\langle a|U|\alpha\rangle = U_{a\alpha}$ and assume $\langle a|U|a\rangle = \langle\alpha|U|\alpha\rangle = 0$.

Making use of the solution of the Dyson equation (6.B.7), and of the relations (6.B.5) and (6.B.6), one can calculate the renormalized state $|\tilde{a}\rangle$ to be employed in working out the modified, single-particle transfer formfactor.

From the secular equation ~~associated with H, namely~~

$$\begin{pmatrix} E_\alpha & U_{a\alpha} \\ U_{a\alpha} & E_a - E_i \end{pmatrix} \begin{pmatrix} C_\alpha(i) \\ C_a(i) \end{pmatrix} = 0, \tag{6.B.4}$$

and associated normalization condition

$$C_a^2(i) + C_\alpha^2(i) = 0, \tag{6.B.5}$$

one obtains

$$C_a^2(i) = \left(1 + \frac{U_{a\alpha}^2}{(E_a - E_i)^2}\right)^{-1}, \tag{6.B.6}$$

and

$$\Delta E_a(E) = E_a - E = \frac{U_{a\alpha}^2}{E_a - E}. \tag{6.B.7}$$

The energy of

~~The relations 6.B.6 and 6.B.7 allows one to write~~ the correlated state

$$|\tilde{a}\rangle = C_a(i)|a\rangle + C_\alpha(i)|\alpha\rangle, \tag{6.B.8}$$

6.B.1

is obtained

~~the corresponding energy being provided~~ by the (iterative) solution of the Dyson equation 6.B.7, which propagate the bubble diagrams shown in Figs ?? (a) and (b) to infinite order leading to collective vibrations (see Fig. ??)

6.B.1 (c)

given in Eq. (6.A.5)

With the help of the definition ??, and making use of the fact that in the present case, $U \equiv \Delta E_a(E)$, one obtains

$$Z_\omega = C_a^2(i) = \left(\frac{m_\omega}{m}\right)^{-1}. \tag{6.B.9}$$

the solution of 6.B.7 together with the relations ?? and ?? lead to the quasiparticle state ??, to be employed in the calculation of the one–particle transfer transition amplitudes (cf. eg. ?? and ??)

Appendix 6.C The Lamb Shift

6.C.1

In Fig. ?? we display a schematic summary of the electron–photon processes, associated with Pauli principle corrections, leading to the splitting of the lowest s, p states of the hydrogen atom known as the Lamb shift.

In the upper part of the figure the predicted position of the electronic single–particle levels of the hydrogen atom as resulting from the solution of the Scrödinger equation (Coulomb field). In the lowest part of the figure one displays the electron of an hydrogen atom (upwards going arrowed line) in presence of vacuum ZPF (electron–positron pair plus photon, oyster–like diagram). Because the associate electron virtually occupies states already occupied by the hydrogen's electron, thus violating Pauli principle, one has to antisymmetrize the corresponding two–electron state. Such process gives rise to the exchange of the corresponding fermionic lines and thus to CO–like digrams as well as, through time ordering, to PO–like diagrams. The results provide a quantitative account of the experimental findings.

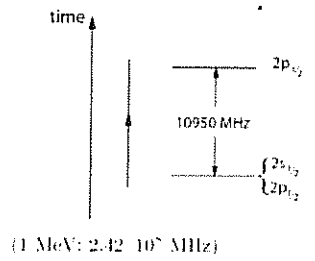

W.E. Lamb, Jr., R.C. Retherford, Phys. Rev. **72** (1947) 241

(1 MeV: 2.42 10^{8} MHz)

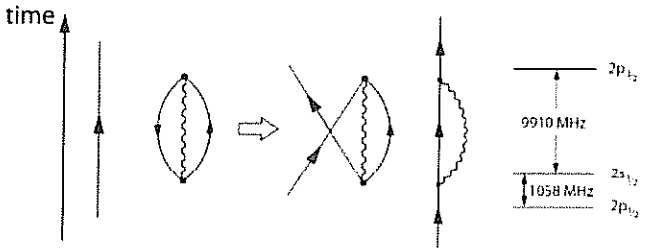

breaking of the s,p level degeneracy

Figure 6.C.1: Schematic representation of the processes associated with the Lamb shift.

Appendix 6.D Self–energy and vertex corrections

In Fig. an example of the fact that in field theories (e.g. QED or NFT), nothing is free and that e.g., the bare masss of a fermion (electron or nucleon), is the parameter one adjusts (m_k) so that the result of a measurement (cf. Fig.) gives the observed mass (single particle energy). In Fig. , lowest order diagrams associated with the renormalization of the fermion–boson interaction (vertex corrections) are given. The sum of contributions (a) and (b) can, in principle, be represented by a renormalized vertex (cf. digram (c) of Fig.). It is of notice, however, that there is, as a rule, conspicuous interference (e.g. cancellation) in the nuclear case between vertex and self–energy contributions (cf. diagrams (e) and (f) of Fig.) a phenomenon closely related with conservation laws (generalized Ward identities)). In particular, cancellation in the case in which the bosonic modes are isoscalar. Consequently, one has to sum explicitly the different amplitudes with the corresponding phases and eventually take the modulus squared of the result to eventually obtain the quantities to be compared with the data, a fact that precludes the use of an effective (renormalized) vertex (cf. Fig.).

Within the framework of QED the above mentioned cancellations are exact implying that the interaction between one and two photon states vanishes (Furry theorem). The physics at the basis of the cancellation found in the nuclear case can be exemplified by looking at a spherical nucleus displaying a low–lying collective quadrupole zero–point vibration. The associated zero point fluctuations (ZPF) lead to time dependent shapes with varied instantaneous values of the quadrupole moment, and of its orientation (dynamical spontaneous breaking of rotational invariance). In other words, a component of the ground state wavefunction ($|(j_p \otimes j_h^{-1})_{2^+} \otimes 2^+; 0^+\rangle$) can be viewed as a gas of quadrupole (quasi) bosons, promoting a nucleon across the Fermi energy (particle–hole excitation) will lead to fermionic states which behave as having a positive (particle) and a negative (hole) effective quadrupole moment, in keeping with the fact that the closed shell system is spherical, thus carrying zero quadrupole moment.

~~Self-Energy (effective-mass) processes~~

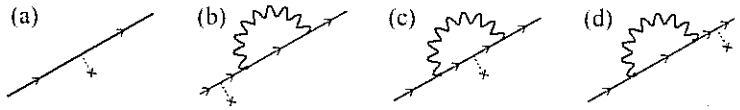

Figure 6.D.1: ~~The~~ result of the probing with an external field (dotted line started with a cross) of ~~the~~ properties (mass, single–particle energy, etc) of a fermion (e.g. an electron or a nucleon, arrowed line) dressed through the coupling of (quasi) bosons (photons or collective vibrations, wavy line), corresponds to the modulus squared of the sum of the amplitudes associated with each of the four diagrams (a)–(d) (cf. Feynman, ~~Theory of fundamental processes~~).

Self-energy (effective-mass-like) processes.

and of the corresponding time-ordering processes

~~Vertex corrections~~

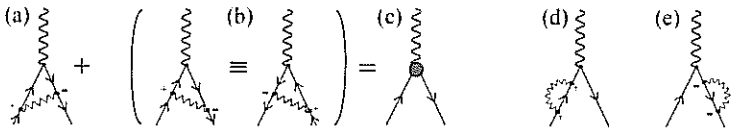

Figure 6.D.2: These are triple–interaction vertex diagrams in which none of the incoming lines can be detached from either of the other two by cutting one line. Migdal's (1958) theorem states that, for phonons and electrons (Bardeen–Pines–Frölich mechanism to break gauge invariance), vertex corrections can be neglected, but usually they are not negligible, in any case not in nuclei (cancellation) (cf. e.g. P.W. Anderson, ~~Basic notions of condensed matter physics~~). The solid circle in (c) represents the effective, renormalized vertex.

Vertex corrections.